On the lowest excited singlet state of osmium tetroxide

K. M. Swift and E. R. Bernstein

On the lowest excited singlet state of osmium tetroxide[a]

K. M. Swift and E. R. Bernstein

Department of Chemistry, Colorado State University, Fort Collins, Colorado 80523

Two-photon spectra of OsO_4 in the region below the first strong one-photon transition are observed and analyzed. The data fit a linear Jahn–Teller $(T \times t)$ calculation. An assignment of the two-photon features as arising from a T_1 electronic state, origin at 27 295 cm^{-1}, with a dominant linear Jahn–Teller active t_2 vibration v_3, $v'_3 = 588$ cm^{-1} $(v''_3 = 960$ cm$^{-1})$, and with Jahn–Teller parameter $D = 0.5$ is proposed. Based on these findings the two observed one-photon states are discussed and qualitatively analyzed in a parallel fashion.

I. INTRODUCTION

Osmium and ruthenium tetroxides (OsO_4, RuO_4) have been the subjects of intense investigation for many years. Ultraviolet absorption,[1-14] photoelectron spectroscopy,[15-17] and magnetic circular dichroism (MCD)[11-13,18] have all been used to probe the electronic structure of these molecules.

OsO_4 and RuO_4 are of interest as members of a large class of tetrahedral, isoelectronic "tetroxo" compounds (MO_4^{n-}; M = Cr, Mo, W, Mn, Tc, Re, Ru, Os). These compounds all show intense dipole allowed transitions in the visible or ultraviolet. For the point group T_d, the dipole operator transforms as T_2, so these allowed states are assigned as being of T_2 symmetry.

There is general consensus that the molecular orbital scheme shown in Fig. 1 holds for these compounds. As shown in the figure, the lowest energy electron promotion $e \leftarrow t_1$ yields both T_1 and T_2 electronic states. The first strong one-photon transition can then be assigned as being of the $e \leftarrow t_1$ type. The t_1 orbital has mainly nonbonding oxygen atomic orbital character. The e orbital is composed mainly of osmium $5d$ orbitals, which have been split by the ligand field into a lower e orbital and upper t_2 orbital. Transitions involving these orbitals are commonly called charge transfer transitions, since an electron is transferred from the oxygen atom to the osmium atom.

The other state arising from the electron promotion $e \leftarrow t_1$, namely, the T_1 state, has been observed for the permanganate ion (MnO_4^-) through careful crystal studies[19,20] and MCD spectroscopy.[21] It is weak and lies well below the first intense transition.

We have investigated the low-lying regions of the OsO_4 spectrum from 25 000–32 300 cm^{-1} using the technique of two-photon gas phase fluorescence excitation spectroscopy in an attempt to find new information about the electronic structure of OsO_4.

II. EXPERIMENTAL

The tunable laser for these experiments was a Nd/YAG pumped dye laser (Quanta-Ray DCR-1A and PDL). Five dyes were necessary to cover the entire range of reported spectra. In order to obtain sufficient power in the low energy region 25 000–28 000 cm^{-1}, it

was necessary to Raman shift (in high pressure H_2) the output of Rhodamine 640, 610, and 590 (Exciton). For the region 27 700–30 100 cm^{-1} a special experimental dye related to DCM was kindly donated to us by Exciton Chemical Company, Inc.; DMSO was the solvent used. For 29 900–32 300 cm^{-1} Exciton DCM was used. In all cases the laser linewidth was roughly 0.3 cm^{-1}.

Spectra were obtained by monitoring emission from the sample following excitation. Input power was between 2–10 mJ/pulse. Emission was detected perpendicular to the focused incident beam by an RCA 8850 photomultiplier tube protected by two Hoya B-390 filters and a 1.0 cm path length of 80% saturated $CuSO_4 \cdot 5H_2O$ in water (250 g/liter). The output of the phototube was put directly into the A channel of a boxcar integrator (PAR 164/162). Dye laser power was monitored by a silicon photodiode, whose output was put directly into the B channel of the boxcar integrator. The spectra were obtained by scanning the dye laser under computer control, and sampling the output of the two channels of the boxcar integrator for several laser pulses at each

MOLECULAR ORBITALS
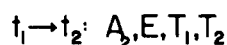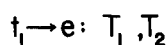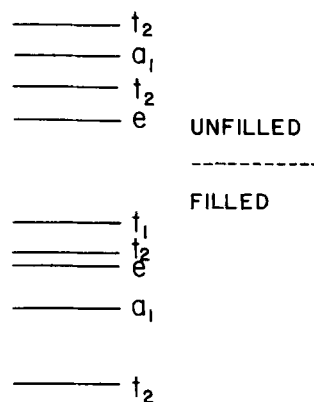
FIG. 1. Molecular orbital scheme for OsO_4. The bottom part of the figure shows the electronic states arising from certain electronic transitions. The lower filled orbitals are drawn to scale and are determined by photoelectron spectroscopy.[17]
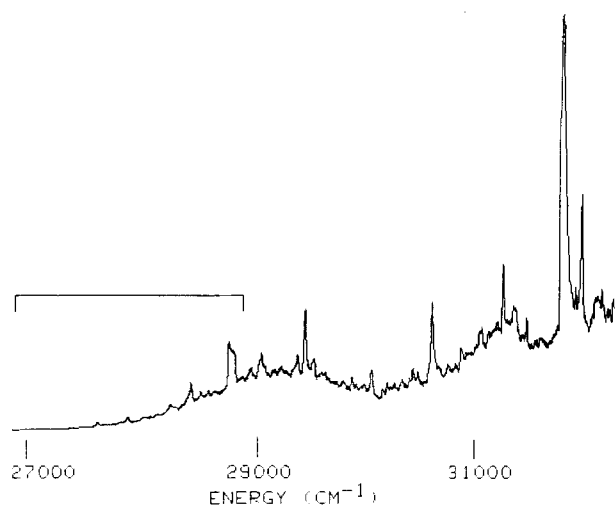
FIG. 2. Survey two-photon photochemiluminescence spectrum of OsO₄. The bracketed area is expanded in Fig. 3. The vertical axis is the total emission intensity normalized to the square of the laser power.

wavelength. Normalization for the square power dependence characteristic of two-photon absorption was accomplished by dividing the signal channel (A) by the square of the power channel (B). In addition, the optogalvanic spectrum of an Fe–Ne hollow cathode lamp was recorded simultaneously for calibration purposes. Between five and 30 scans over the dye's range were averaged, depending on the signal to noise ratio. Circularly polarized light was obtained with a Fresnel rhomb.

The material used was commercial OsO₄, purified further by distillation under high vacuum through a 4 Å molecular sieve. OsO₄ reacts with grease, so a grease free vacuum manifold was used. The sample cell was filled with the full vapor pressure at room temperature
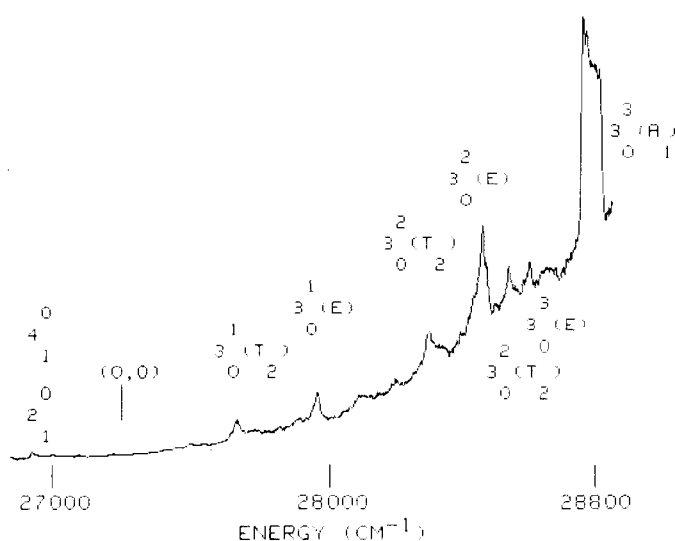
FIG. 3. First 2000 cm⁻¹ of the two-photon photochemiluminescence spectrum of OsO₄. Assignments for this region, given by a linear Jahn–Teller calculation, label various features. The vertical axis is total emission intensity normalized to the square of the laser power.

TABLE I. Tabulation and assignment of observed two photon energy levels of OsO₄ T_1 first excited electronic state.

$2\sigma_{vac}$ (cm⁻¹)	Intensity[a]	Assignment
26 805	VW	
26 965	W	$2_1^0 (T_1 \leftarrow E)$, $4_1^0 (T_1 \leftarrow T_2)$
27 041	VW	
27 141	VW	
27 568	VW	$2_0^1 (T_2)$ or $4_0^1 (T_2)$
27 745	M	$3_0^1 (T_2)$
27 790	VW	
27 955	VW	
27 984	M	$3_0^1 (E)$
28 108	VW	
28 217	VW	
28 316	W	$3_0^2 (T_2)$
28 483	M	$3_0^2 (E)$
28 562	W	$3_0^2 (T_2)$
28 627	W	$3_0^3 (E)$
28 792[b]	S	$3_0^3 (A_1)$
28 843[b]	S	
28 981	M	$3_0^3 (T_2)$
29 054[b]	S	
29 069	S	$3_0^3 (E)$
29 160	M	
29 182	M	
29 235	M	
29 373	S	
29 440	VS	
29 517	S	
29 771	M	
29 848	M	
30 025	S	
30 119	M	
30 161	M	
30 226	M	
30 298	M	
30 363	M	
30 403	M	
30 447	M	
30 582	VS	
30 729	M	
30 850	M	
31 028	M	
31 054	M	
31 197	M	
31 254	VS	
30 358	S	
31 381	S	
31 486	M	
31 827[b]	VVS	$3_0^1 (A_1)$ [T_2]
31 974	M	
32 034	VS	
32 171	M	
32 241	M	

[a]W = weak, VW = very weak, M = medium, S = strong, VS = very strong, VVS = very very strong.
[b]Changes intensity with circularly polarized light.

(21 °C). Vapor pressure was measured to be about 5 Torr with a Baratron gauge.

III. RESULTS AND DISCUSSION

The observed spectrum is shown in survey form in Figs. 2 and 3 and the complete data are tabulated in Table I. There are no features until about 26 800 cm⁻¹,

TABLE II. Polarization and selection rules for two-photon transitions in T_d symmetry.

Vibronic symmetry	ΔK selection rule	Polarization behavior
$A_1 \leftarrow A_1$	$\Delta K = 0$	Completely polarized
$E \leftarrow A_1$	$\Delta K = 0, \pm 2$	Unpolarized
$T_2 \leftarrow A_1$	$\Delta K = \pm 1, \pm 2$	Unpolarized

at which point a very complicated spectrum begins. The spectrum extends into the region of the first strong one-photon state which begins at 31 359 cm⁻¹.[8]

In an attempt to elucidate the vibrational parentage of the transitions, emission from the sample excited at two pump energies of 31 830 and 30 582 cm⁻¹ was dispersed in a 1 m monochromator. Emission was found not to be from the molecule OsO₄ but from neutral osmium atoms [Os(I)]. No molecular emission could be found. Still, the excitation spectra that were obtained could be genuine two-photon OsO₄ spectra, if in fact the rate-limiting step for the dissociation followed by emission is the initial two-photon absorption by OsO₄.

This situation is not without precedent. For example, pyrazine and triazine two-photon spectra have been obtained by monitoring the emission from cyanyl (CN) produced by photodecomposition of the sample by the laser.[22,23] However, the possibility of contamination of the spectrum by the photoproducts exists. Thus, the spectrum must be analyzed as OsO₄ in order to prove that it is entirely due to OsO₄.

In order to assign the spectrum, we must consider the two-photon selection rules. McClain and Harris have given an excellent treatment of this problem.[24] Properties of the two-photon transition tensor give both selection rules and polarization behavior. In short, the transition is allowed for identical photons if the transition tensor is symmetric; it is circularly polarized if the tensor has a nonzero trace. These results are applied to the group T_d in Table II. Also contained in Table II are the ΔK selection rules obtained by the method given by McClain and Harris.

Rotational contours can be quite useful for symmetric top assignments, since a one to one correspondence exists between ΔK selection rules and vibronic symmetry.[25,26] For the spherical top, on the other hand, the K levels are degenerate; thus, for a given energy, symmetric top intensity factors must be summed subject to ΔK selection rules. In the notation of Ref. 26,

$$|J'\rangle \leftarrow |J\rangle: \quad W = \sum_{KK'} W_{J'K',JK} = \sum_{KK'}(C_0 M_0 R_0 + C_2 M_2 R_2) \ ,$$

in which $R_0 = \delta_{JJ'} \delta_{KK'}$ and $R_2 = b^{JK}_{J'K'}$, the Placzek–Teller coefficient.[27]

Summation of symmetric top factors is accomplished using the following relations:

$$\sum_{KK'} \delta_{JJ'} \delta_{KK'} = (2J+1)\delta_{JJ'}$$

$$\sum_K b^{JK}_{J'K'} = (2J'+1)/5 \quad \text{(for a given } \Delta K\text{)}.$$

The latter relation is first derived in Ref. 27. The result is that the formulas for the intensity work out similarly for $E \leftarrow A_1$ and $T_2 \leftarrow A_1$:

$$E \leftarrow A_1: \quad W = (C_2/5)(2J'+1)(|M^2_{+2}|^2 + |M^2_{-2}|^2 + |M^0_0|^2) \ ,$$

$$T_2 \leftarrow A_1: \quad W = (C_2/5)(2J'+1)$$
$$\times (|M^2_{+2}|^2 + |M^2_{-2}|^2 + |M^2_{+1}|^2 + |M^2_{-1}|^2) \ ,$$

$$A_1 \leftarrow A_1: \quad W = C_0(2J+1)|M^0_0|^2 \ .$$

Rotational contours can thus distinguish between $A_1 \leftarrow A_1$ and $E \leftarrow A_1$ or $T_2 \leftarrow A_1$, but not between $E \leftarrow A_1$ and $T_2 \leftarrow A_1$.

Expressions for the energy and Coriolis coupling of a spherical top may be found in Refs. 28 and 29. Employing these formulas, calculation of rotational contours proceeds in the standard fashion.[25,26] A linewidth of 2–4 cm⁻¹ was employed for each rotational transition. Some experimental and theoretical rotational con-
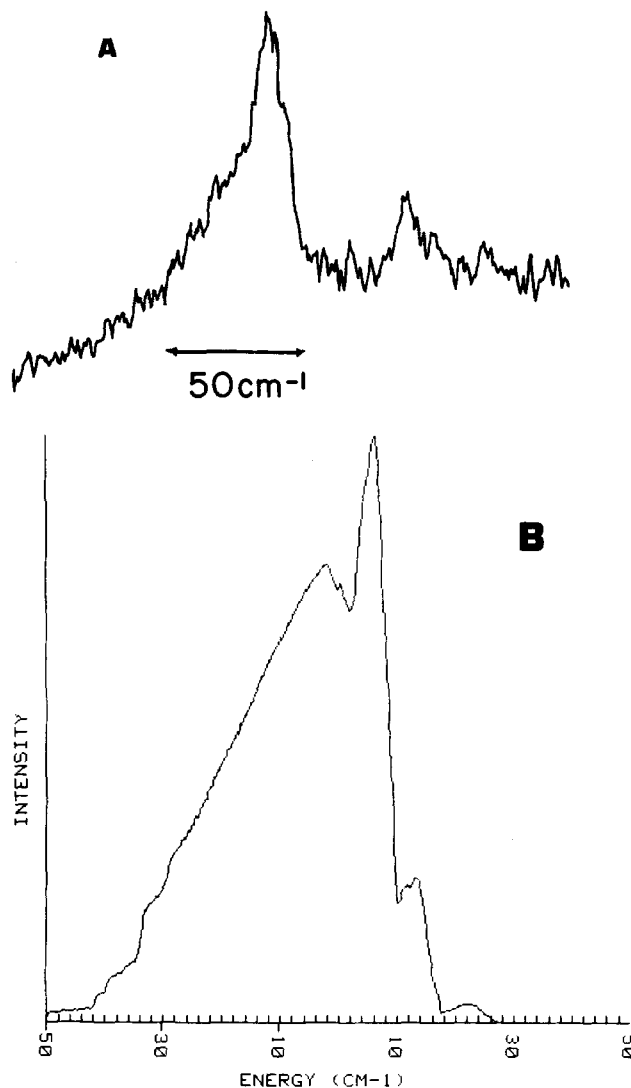

FIG. 4. Rotational contour for $3^1_0 (T_2)$. (a) Experimental, single scan of the feature. Weak peak to high energy side of 3^1_0 is not part of the 3^1_0 contour. (b) Calculated contour with $B'' = 0.1349$ cm⁻¹, $B' = 0.13$ cm⁻¹, $\zeta = -0.6$.

A

$\longleftrightarrow$
50 cm^{-1}

B

INTENSITY

ENERGY (CM-1)

C

INTENSITY

ENERGY (CM-1)

D

INTENSITY

ENERGY (CM-1)
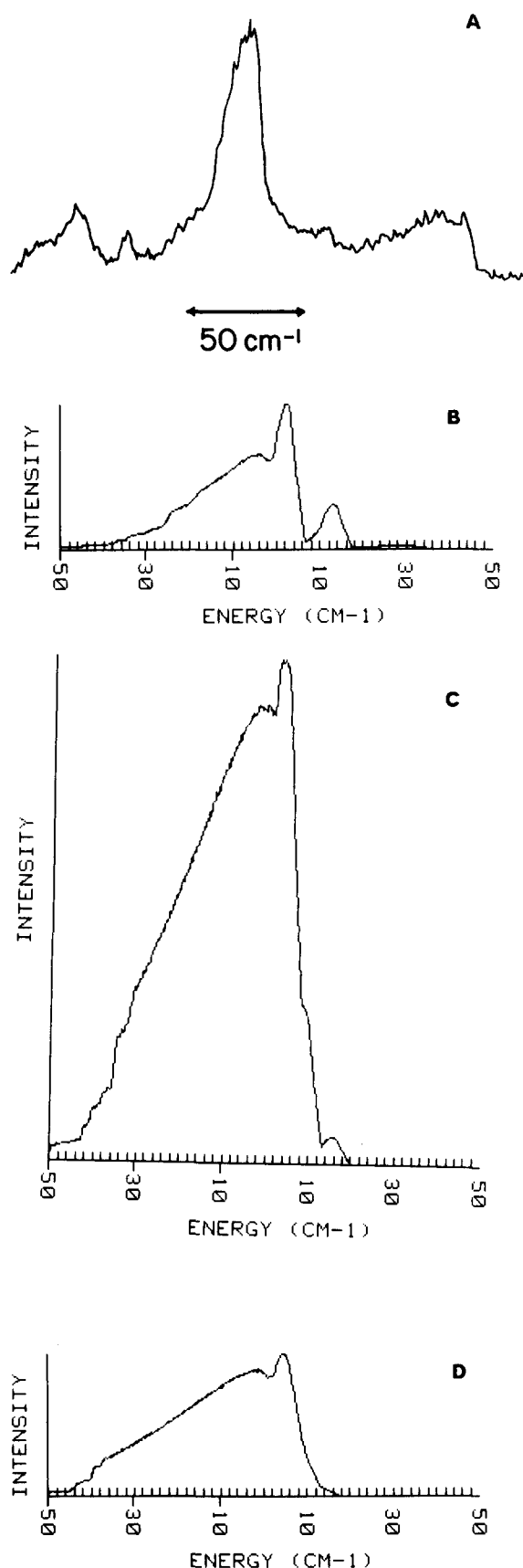
FIG. 5. Rotational contours for 29 373, 29 440, and 29 517 cm^{-1} features: (a) Experimental features, single scan. (b) Calculated for the feature at left—$B'' = 0.1349$ cm^{-1}, $B' = 0.13$ cm^{-1}, $\zeta = -1.0$. (c) Calculated for the central feature—$B'' = 0.1349$ cm^{-1}, $B' = 0.128$ cm^{-1}, $\zeta = -0.6$. (d) Calculated for the feature on the right $B'' = 0.1349$ cm^{-1}, $B' = 0.128$ cm^{-1}, $\zeta = -0.4$.

tours are presented in Figs. 4–6. Note that the experimental contours extend over about 50 cm^{-1}. This would seem to eliminate the possibility of atomic two-photon absorption spectra arising from photogenerated atomic species [Os(I)], such as was reported in Refs. 30 and 31.

It is clear that calculated contours of $3_0^1(T_2)$ (Fig. 4) and the 29 373, 29 440, and 29 517 cm^{-1} features (Fig. 5) agree only fairly well with the experimental ones. The experimental bands are somewhat simpler than the calculated ones. This situation occurs for some of the other features as well. There are three mechanisms which can increase the experimental linewidths: lifetime broadening associated with the photochemistry observed in this region, laser linewidth (~ 0.3 cm^{-1}), and effects due to the presence of multiple isotopes. Os-

A

28770   28870

ENERGY (cm^{-1})

B

INTENSITY
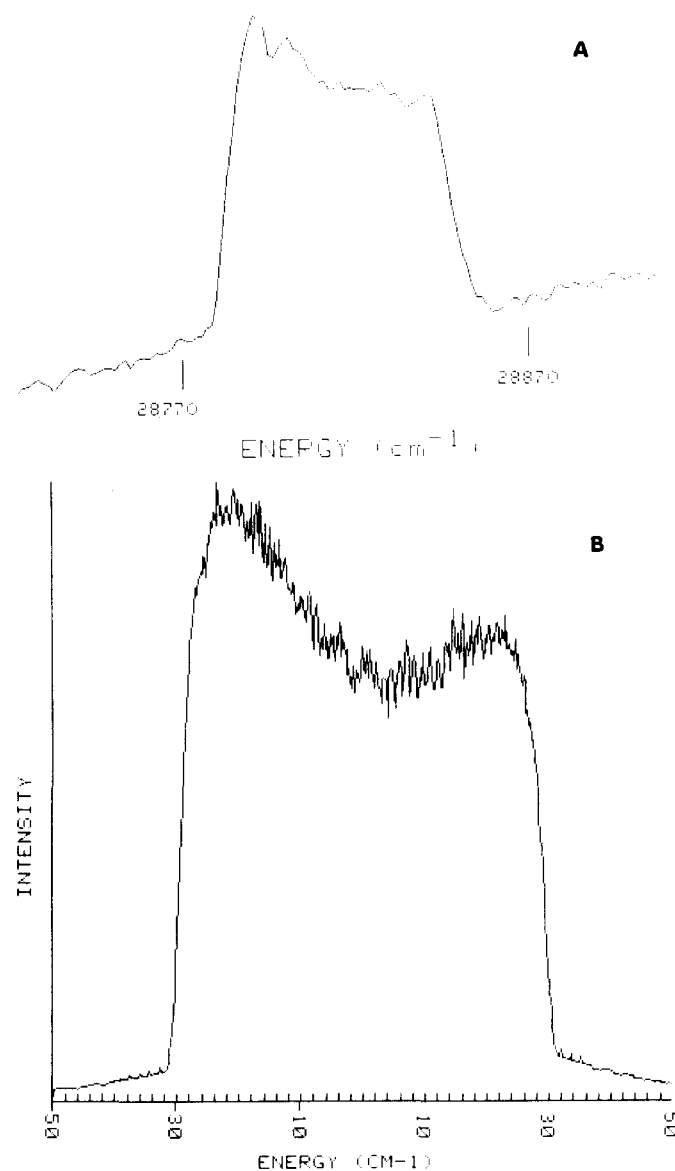
ENERGY (CM-1)

FIG. 6. Rotational contour for 3_0^3 (A_1): (a) Experimental (seven scans). (b) Calculated with two overlapping A_1 bands, the lower one is probably 3_0^3 (A_1)—$B'' = 0.1349$ cm^{-1}, $B_1' = 0.145$ cm^{-1}, $B_2' = 0.125$ cm^{-1}, with origins separated by 60 cm^{-1}. Higher energy contour weighted with an intensity factor of 0.7 that of the lower energy contour.

FIG. 7. Vibronic energy levels for $T_2 \times t_2$ from Ref. 32. For a T_1 electronic state all 1 and 2 subscripts are interchanged. The vertical axis is in units of $\hbar\omega$.

mium has four abundant isotopes: ^{188}Os, ^{189}Os, ^{190}Os, and ^{192}Os. The difference between ν_3 for ^{188}OsO4 and for ^{192}OsO4 is expected to be about 1 cm^{-1}. It should be noted that a diatomic or triatomic symmetric top model, which might be appropriate for photoproduct absorption, generates a poorer rotational contour fit in all instances.

TABLE III. Comparison of observed and calculated[32] ν_3 (t_2) vibronic components in the lowest excited T_1 electronic state of OsO4 (in cm^{-1}). Parameter values are $\nu_3' = 588$ cm^{-1} and $k = 1.0$ $(D = 0.5)$.

Assignment	Observed	Calculated[a]	$n=1$ Eigenvector coefficient[a]
$4^0_1(T_1 \leftarrow T_2)$ $2^0_1(T_1 \leftarrow E)$	26 965	[26 965][b]	...
$(0, 0)$	[27 295][c]	27 295	...
$3^1_0(T_2)$	27 745	27 746	0.708 57
$3^1_0(E)$	27 984	27 978	0.640 57
$3^2_0(T_2)$	28 316	28 314	0.187 14
$3^2_0(E)$	28 483	28 488	0.588 02
$3^2_0(T_2)$	28 562	28 559	0.427 60
$3^3_0(E)$	28 627	28 642	0.368 91
$3^3_0(A_1)$[d]	28 792	28 809	0.633 08
$3^3_0(T_2)$	28 981	28 942	−0.092 403
$3^3_0(E)$	29 069	29 081	−0.274 11

[a]Values supplied by R. Englman; see Ref. 32.
[b]Calculated by subtracting 330 cm^{-1} from origin.
[c]Forbidden; calculated from hot bands 2^0_1, 4^0_1.
[d]Observed and predicted to be polarized.

TABLE IV. Ground state OsO4 vibrations.[a]

			(cm^{-1})
ν_1	a_1	Symmetric stretch	965
ν_2	e	Bend	333
ν_3	t_2	Antisymmetric stretch	960
ν_4	t_2	Bend	329

[a]R. S. McDowell and M. Goldblatt, Inorg. Chem. 10, 625 (1971).

To fit the feature at $\sim 28\,800$ cm^{-1} it was necessary to overlap two totally symmetric contours of different excited-state moments of inertia with origins separated by 60 cm^{-1} (Fig. 6). In fact, the lower energy feature has a moment of inertia 7% larger than the ground state and the high energy feature has a moment of inertia 7% lower than the ground state. Such changes are typical of Jahn–Teller perturbed systems and have been noted before.[23] The agreement between the overlapped calculated contours and the experimental feature is quite reasonable. (See the discussion below.)

The strongest argument for the spectrum being due to OsO4 is that the first nine major features fit the Jahn–Teller $(T_1 \times t_2)$ vibronic calculation of Caner and Englman[32] nearly exactly (average deviation = 11 cm^{-1}) for a parameter value $k = L/\sqrt{6}\,\hbar\omega = 1.0$ or $D = 0.5$ (see Fig. 7). For a comparison of calculated and experimental features, refer to Table III. The value of the unperturbed excited state frequency is 588 cm^{-1}, so the vibration is most likely ν_3', whose ground state frequency is 960 cm^{-1} (see Table IV). The other t_2 vibration ν_4 is probably too low in energy (329 cm^{-1} in the ground state) to be considered for this series. This conclusion is further supported by discussion in the ensuing paragraphs.

Two other pieces of information fit in well with the above interpretation. First, the seventh peak in the progression (28 792 cm^{-1}) is polarized, in accordance with the calculated feature of A_1 symmetry predicted to lie at 28 809 cm^{-1}. As was mentioned earlier, the contour is a combination of two polarized features. We assume that the lower one is $3^3_0(A_1)$. Second, the forbidden T_1 origin is predicted to lie at 27 295 cm^{-1}, and a ~ 330 cm^{-1} hot band appears to be built on this position as it should be, since $2^0_1(T_1 \leftarrow E)$ and $4^0_1(T_1 \leftarrow T_2)$ will be allowed. Hot bands located 330 cm^{-1} below the major features are not generally found, however, presumably because they involve a change in quanta for two vibrations, ν_3 and ν_2 or ν_4. The Boltzmann factor for ν_3 hot bands is very unfavorable.

Intensities for the $[T_1 \times t_2]$ ν_3 manifold are qualitatively in agreement with the $n=1$ coefficients of the computed eigenvectors, as would be expected for a Herzberg–Teller vibronic coupling intensity mechanism.[23] For example, the following predictions (see Table III) can be accurately made: $3^3_0(A_1)$ at $\sim 28\,800$ cm^{-1} is quite intense; $3^2_0(T_2)$ at 28 316 cm^{-1} is less intense than $3^2_0(E)$ at 28 483 cm^{-1}; and $3^3_0(T_2)$ at 28 981 cm^{-1} is less intense than $3^3_0(E)$ at 29 069 cm^{-1}. Other trends in these data are also predicted correctly by the eigenvector calculations.

Thus, nine energies and intensities, plus two additional pieces of information, are fit by two parameters (the linear Jahn–Teller coupling strength and the excited frequency). The fact that one vibration should dominate the entire spectrum is similar to the situation in triazine, for which ν_6 dominates the spectrum.[23] What is unusual here, however, is the absence of any obvious totally symmetric progression built on the ν_3 series. Features above the one at 29 069 cm^{-1} are difficult to assign to specific ν_3 components since at these higher energies there are many states arising from a degenerate vibration. Moreover, calculation of the upper levels is less accurate since the basis includes only the lower harmonic oscillator functions. Some features may be one quantum of the totally symmetric vibration ν_1 built on the lower ν_3 features, but longer ν_1 progressions are not apparent.

The one-photon spectrum also lacks a well defined totally symmetric progression,[8] though at first glance the spectrum appears to possess a long series in ν_1. It may be that ν_3 perturbs the one-photon spectrum as well. In fact, the first six $T_2 \times t_2$ vibronic coupling calculation T_2 levels actually fit the first few one-photon features fairly well (average deviation 43 cm^{-1}) for a parameter value $k = L/\sqrt{6}\,\hbar\omega = 1.0$ or $D = 0.5$ and ν_3' $= 736$ cm^{-1} (see Table V). This good agreement indicates that ν_3 is involved in the progression in the lower T_2 state. These conclusions are consistent with those reached through MCD studies of both MnO$_4^-$[33] and OsO$_4$.[11,12] The value of the Jahn–Teller parameter for the lower T_2 state is about a factor of 2 larger than that of MnO$_4^-$ $(D = 0.27)$.[33]

Our two-photon data also support this conclusion, as there is an intense polarized feature at 31 827 cm^{-1} and the calculation gives a one-photon forbidden A_1 vibronic symmetry feature at 31 846 cm^{-1}. This is the only predicted A_1 $[T_2 \times t_2]$ level within ± 1000 cm^{-1} of the observed feature.

TABLE V. Comparison of one-photon data[8] for the T_2 state of OsO$_4$ with the vibronic coupling $T_2 \times t_2$ calculation[32] $(D = 0.5, \nu_3' = 736$ cm$^{-1})$. sh, shoulder; p, peak. Frequencies in cm^{-1}. Error in frequencies 5–20 cm^{-1}.

Band[a]	Observed	Calculated[c]
A	31 261 sh	
	31 359 p	31 294 (T_2)
	31 398 sh	
A–B	31 661 sh	
	[31 827 p (A_1)][b]	31 846 (A_1)
B	32 093 sh	
	32 197 p	32 305 (T_2)
B–C	32 479 p	32 489 (T_2)
C	32 950 sh	32 931 (T_2)
	33 059 p	33 041 (T_2)
C–D	33 297 p	33 262 (T_2)

[a]Reference 8 band designations.
[b]Observed two-photon peak, this work.
[c]Measured from Ref. 32 figure (± 20 cm^{-1}).

TABLE VI. Comparison of one-photon data[8] for the upper T_2 state of OsO$_4$ with vibronic coupling T_2 $\times t_2$ calculation[32] $(D = 1.1, \nu_3' = 754$ cm$^{-1})$. sh, shoulder; p, peak. Frequencies in cm^{-1}. Error in frequencies 5–20 cm^{-1}.

Band[a]	Observed	Calculated[b]
K	38 421 sh	
	38 509 sh	
	38 643 sh	
	38 733 p	38 743
	38 906 sh	
K–L	39 112 sh	
L	39 381 sh	
	39 523 sh	
	39 592 p	39 573
	39 765 p	39 742
L–M	40 100 sh	40 139
M	40 433 p	40 478
	40 605 p	40 553

[a]Reference 8 band designations.
[b]Measured from Ref. 32 figure (± 20 cm^{-1}). All features T_2.

One can then examine the second intense one-photon transition beginning at 38 733 cm^{-1} for possible agreement with the calculation. For $D = 1.1$ and $\nu_3' = 754$ cm^{-1}, one again finds agreement (see Table VI) with an average deviation of 31 cm^{-1}. We therefore believe that the irregularities in the progression intervals in the one-photon data are due to a linear Jahn–Teller perturbed $\nu_3'(t_2)$ manifold in both T_2 electronic states. However, due to the diffuse nature of the one-photon spectrum, conclusive proof for this apparently reasonable conclusion must await further spectroscopic studies now in progress.

The ν_3 vibration involves the central osmium atom moving in one direction, with the oxygen atoms moving in the opposite direction. The mode is the only one involving movement of the osmium atom. Therefore, it is to be expected that ν_3 would be quite important for vibronic coupling (both Herzberg–Teller and Jahn–Teller) in a charge transfer transition.

We are continuing the investigation of two-photon features in the one-photon region. We also plan to employ the photoacoustic detection method in order to gain further information with regard to the photophysics and photochemistry of this system.

IV. CONCLUSIONS

A low lying T_1 state of OsO$_4$ has been observed by two-photon spectroscopy. The spectrum is dominated by a Jahn–Teller perturbed $\nu_3(t_2)$ vibrational progression. This interpretation is strongly supported by the $T_1 \times t_2$ vibronic coupling calculation of Caner and Englman, which gives the location of the T_1 electronic origin as 27 295 cm^{-1}, $\nu_3' = 588$ cm^{-1}, and $D = 0.5$. Both one-photon allowed T_2 states are also qualitatively inter-

pretable in terms of these concepts. Finally, OsO_4 is observed to be photochemically active, producing neutral osmium atoms which then emit.

ACKNOWLEDGMENT

[1] J. Lifschitz and E. Rosenbohm, Z. Phys. Chem. 97, 1 (1921).

[2] S. Kato, Sci. Pap. Inst. Phys. Chem. Res. (Jpn.) 13, 249 (1930).

[3] A. Langseth and B. Qviller, Z. Phys. Chem. Abt. B 27, 79 (1934).

[4] S. E. Krasikov, A. N. Filippov, and I. I. Chernyaev, Izv. Sekt. Platiny Drugikh Blagorodn. Met. Inst. Obshch. Neorg. Khim. Akad. Nauk SSSR 13, 19 (1936).

[5] B. Qviller, Tidsskr. Kjemi Bergves. Metall. 17, 127 (1937).

[6] R. E. Connick and C. R. Hurley, J. Am. Chem. Soc. 74, 5012 (1952).

[7] G. B. Barton, Spectrochem. Acta 19, 1619 (1963).

[8] E. J. Wells, A. D. Jordan, D. S. Alderdice, and I. G. Ross, Aust. J. Chem. 20, 2315 (1967).

[9] A. Mueller and E. Diemann, Chem. Phys. Lett. 9, 369 (1971).

[10] S. Foster, S. Felps, L. W. Johnson, D. B. Larson, and S. P. McGlynn, J. Am. Chem. Soc. 95, 6578 (1973).

[11] T. J. Barton, R. Grinter, and A. J. Thomson, Chem. Phys. Lett. 40, 399 (1976).

[12] P. Quested, D. J. Robbins, P. Day, and R. G. Denning, Chem. Phys. Lett. 22, 158 (1973).

[13] R. H. Petit, B. Briat, A. Mueller, and E. Diemann, Mol. Phys. 27, 1373 (1974).

[14] W. H. Beattie, W. B. Maier, R. F. Holland, S. M. Freund, and B. Stewart, SPIE Proc. 158, 113 (1978).

[15] E. Diemann and A. Mueller, Chem. Phys. Lett. 19, 538 (1973).

[16] S. Foster, S. Felps, L. C. Cusachs, and S. P. McGlynn, J. Am. Chem. Soc. 95, 5521 (1973).

[17] P. Burroughs, S. Evans, A. Hamnett, A. F. Orchard, and N. V. Richardson, J. Chem. Soc. Faraday Trans. 2 70, 1895 (1974).

[18] R. H. Petit, B. Briat, A. Mueller, and E. Diemann, Chem. Phys. Lett. 20, 540 (1973).

[19] P. Day, L. Disipio, and L. Oleari, Chem. Phys. Lett. 5, 533 (1970).

[20] L. W. Johnson, E. Hughes, Jr., and S. P. McGlynn, J. Chem. Phys. 55, 4476 (1971).

[21] J. C. Collingwood, P. Day, R. G. Denning, D. J. Robbins, L. Disipio, and L. Oleari, Chem. Phys. Lett. 13, 567 (1972).

[22] J. D. Webb, K. M. Swift, and E. R. Bernstein, J. Mol. Struct. 61, 285 (1980).

[23] J. D. Webb, K. M. Swift, and E. R. Bernstein, J. Chem. Phys. 73, 4891 (1980).

[24] W. M. McClain and R. A. Harris, in Excited States, edited by E. C. Lim (Academic, New York, 1977), Vol. 3, pp. 1—56.

[25] L. Wunsch, F. Metz, H. J. Neusser, and E. W. Schlag, J. Chem. Phys. 66, 386 (1977).

[26] F. Metz, W. E. Howard, L. Wunsch, H. J. Neusser, and E. W. Schlag, Proc. R. Soc. London Ser. A 363, 381 (1978).

[27] G. Placzek and E. Teller, Z. Phys. 81, 209 (1933).

[28] H. C. Allen Jr. and P. C. Cross, Molecular Vib-Rotors (Wiley-Interscience, New York, 1963).

[29] F. N. Masri and W. H. Fletcher, J. Chem. Phys. 52, 5759 (1970).

[30] D. P. Gerridy, L. J. Rothberg, and V. Vaida, Chem. Phys. Lett. 74, 1 (1980).

[31] S. Leutwyler, U. Even, and J. Jortner, Chem. Phys. Lett. 74, 11 (1980).

[32] R. Englman, The Jahn—Teller Effect in Molecules and Crystals (Wiley-Interscience, New York, 1972), p. 72.

[33] P. A. Cox, D. J. Robbins, and P. Day, Mol. Phys. 30, 405 (1975).